J. Basic. Appl. Sci. Res., 3(7)656-666, 2013
© 2013, TextRoad Publication
ISSN 2090-4304
Journal of Basic and Applied Scientific Research
www.textroad.com

Numerical Simulation of Three-Dimensional Supersonic Flow around an Aerodynamic Bump.

Ahmed Kadhim Hussein[1,*], Waqar Ahmed Khan[2], S.Sivasankaran[3], H. A. Mohammed[4], I.K.Adegun[5]

[1]College of Engineering -Mechanical Engineering Department - Babylon University- Babylon City – Hilla – Iraq.
[2]National University of Sciences and Technology - Department of Engineering Sciences - PN Engineering College PNS Jauhar , Karachi 75350, Pakistan
[3] Institute of Mathematical Sciences, University of Malaya, Kuala Lumpur 50603, Malaysia
[4] Department of Thermofluids, Faculty of Mechanical Engineering ,Universiti Teknologi Malaysia (UTM), 81310 UTM Skudai, Johor Bahru, Malaysia
[5] Department of Mechanical Engineering, University of Ilorin, Ilorin, Nigeria

ABSTRACT

This study is used to compute the primitive variables of moderate supersonic flow based on finite difference computational fluid dynamic methods. The problem considered deals with a three-dimensional external, inviscid ,compressible supersonic flow over a three-dimensional arc circular bump. In this work, Euler equation was solved using time-marching Mac Cormack's explicit technique. The flow conditions are taken at sea level and Mach number at **1.97**. To deal with complex shape of arc circular bump the so-called "body fitted coordinate system" were considered and the algebraic methods were used to generate grids over an arc circular bump. The results showed a good agreement with other published results.

KEYWORDS: Arc circular bump , CFD , Supersonic aerodynamics, Euler equation.

1. INTRODUCTION

Supersonic flow was a flow in which a Mach number is greater than **1.0**, and this flow is very important in the design of aircraft and rockets. During the past, the experimental and analytical methods were used to simulate the properties of supersonic flow over a limited number of shapes, but for supersonic three-dimensional shapes such as a **3D** arc circular bump, the analytical method was failed due to non-linearity also to design an aircraft many thousands of tests were drawn in a supersonic wind tunnel which requires a hard and expensive work and require a very long time. In contrast, a numerical prediction give the same result with a short-time and an accurate computation and the computer program may be changed easily to deal with any other complex shape such as wing, airfoil and missile **AL-Dulaimy (2002)** .In the numerical simulation, the complex differential equations are overcame by replacing it with differences, calculated from a finite number of values associated with the computational nodes, which are distributed on a suitable grid over the solution domain. In the present study, the predictor-corrector MacCormack's explicit finite difference method with time marching was adopted to predict the aerodynamic characteristics of three-dimensional external compressible inviscid supersonic flow over an arc circular bump to compute the primitive variables such as the internal energy, pressure, density, Mach number and temperature at each grid. The time- marching method was chosen to treat an arc circular bump as a plane body. In the next section, the mathematical analysis will be described in detail and the style, which used to produce meshes or grids are given. It is very important to refer that the primitive variable covers, velocity, density, temperature, pressure, internal energy and Mach number.

4.Mathematical Analysis: The studied supersonic flow is a non-viscous, non-heat conducting fluid, so it is described by **Euler equation**. The latter is obtained from **Navier-Stokes** equations by neglecting all shear stresses and heat-conduction terms, so it is a valid approximation for flows at high speed (supersonic flow), i.e., at high Reynolds number outside the viscous region developing near the solid surface. The mathematical behavior of the Euler equation is classified as hyperbolic in supersonic flow **Hosseini (2006)**. The solution is obtained using time-marching method. In this method two points must be noticed.

1. The grid points are generated in physical plane and transformed to computational plane before solving governing equations.
2. The solution is obtained by marching from some initial flow field through time until a steady – state is obtained.

The governing equations for an inviscid, non-heat conducting, external, compressible, three-dimensional supersonic flow expressed in conservation form are **Hoffmann (1989):**

Continuity equation:

$$\nabla.(\rho V) = \frac{\partial \rho}{\partial t} + \frac{\partial(\rho u)}{\partial x} + \frac{\partial(\rho \upsilon)}{\partial y} + \frac{\partial(\rho w)}{\partial z} \qquad \text{...(1)}$$

[*]**Corresponding Author:** Ahmed Kadhim Hussein, College of Engineering-Mechanical Engineering Department- Babylon University- Babylon City – Hilla – Iraq. E-mail addresses: ahmedkadhim74@yahoo.com

The conservation of momentum equation is :

$$\frac{\partial(\rho u)}{\partial t}+\frac{\partial(\rho u^2+p)}{\partial x}+\frac{\partial(\rho u v)}{\partial y}+\frac{\partial(\rho u w)}{\partial z}=0$$

$$\frac{\partial(\rho v)}{\partial t}+\frac{\partial(\rho u v)}{\partial x}+\frac{\partial(\rho v^2+p)}{\partial y}+\frac{\partial(\rho v w)}{\partial z}=0$$

$$\frac{\partial(\rho w)}{\partial t}+\frac{\partial(\rho u w)}{\partial x}+\frac{\partial(\rho w v)}{\partial y}+\frac{\partial(\rho w^2+p)}{\partial z}=0 \qquad \text{…(2)}$$

The **conservation of energy equation** is :

$$\frac{\partial(\rho E_t)}{\partial t}+\frac{\partial}{\partial x}[(\rho E_t+p)u]+\frac{\partial}{\partial y}[(\rho E_t+p)v]+\frac{\partial}{\partial z}[(\rho E_t+p)w]=0 \qquad \text{…(3)}$$

It is suitable to put these equations in a vector form before applying a numerical scheme to these equations. The 3-dimensinal Euler equation may be arranged in a vector form as **Hoffmann (1989)**

$$\frac{\partial Q}{\partial t}+\frac{\partial E}{\partial x}+\frac{\partial F}{\partial y}+\frac{\partial G}{\partial z}=0 \qquad \text{…(4)}$$

where Q,E,F and G are column vectors which is defined by:

$$Q=\frac{\partial}{\partial t}=\begin{bmatrix}\rho\\ \rho u\\ \rho v\\ \rho E_t\end{bmatrix};\ E=\frac{\partial}{\partial x}=\begin{bmatrix}\rho u\\ \rho u^2+P\\ \rho u v\\ (\rho E_t+P)u\end{bmatrix};\ F=\frac{\partial}{\partial y}=\begin{bmatrix}\rho v\\ \rho u v\\ \rho v^2+P\\ (\rho E_t+P)v\end{bmatrix};\ G=\frac{\partial}{\partial z}=\begin{bmatrix}\rho w\\ \rho u w\\ \rho w^2+P\\ (\rho E_t+P)w\end{bmatrix} \qquad \text{…(5)}$$

also the equation of state is given by :-

$p=\rho RT$, at ambient temperature, it becomes :-

$$\rho_\infty=\frac{p_\infty}{RT_\infty} \qquad \text{…(6)}$$

and the speed of sound is given by :-

$$a_\infty=\sqrt{\gamma RT_\infty}$$

The total pressure and temperature (or stagnation pressure and temperature) are given by: -

$$p_o=p_\infty\left[1+\frac{(\gamma-1)}{2}M^2\right]^{\frac{\gamma}{\gamma-1}} \qquad \text{…(7)}$$

$$T_o=T_\infty\left[1+\frac{(\gamma-1)}{2}M^2\right] \qquad \text{…(8)}$$

The Reynolds number and boundary layer thickness are given by :-

$$\mathrm{Re}=\frac{\rho_\infty u_\infty L}{\mu_\infty} \quad \text{and} \quad \delta=\frac{5.0L}{\mathrm{Re}_L^{0.5}} \qquad \text{…(9)}$$

Moreover the velocity components are given by :-

$$u_\infty=V\cos\alpha \qquad \text{…(10-A)}$$

$$v_\infty=V\sin\alpha \qquad \text{…(10-B)}$$

where $V=M\,a_\infty$ noting that:-

M=Mach number. and a_∞ = speed of sound.

V =Fluid velocity.

δ =Boundary layer thickness.

Re=Reynolds number.

μ_∞ =Free stream dynamic viscosity.

5.Three- Dimensional Mesh Generation:

In this work, the **algebraic grid generation** method is used to produce mesh. This method generates grid points in space by means of interpolations based on given boundary data. Because of the non-uniform shape of arc circular bump, a " body-fitted coordinate system " is used which enable us for the transformation of governing equations from a Cartesian system **(x ,y,z)** to a general curvilinear system **(** ζ, η, ξ **)** and it help us to transform from **physical plane** to the **computational plane Fox (1993)**.The transformation of any partial differential equations from physical plane **(x, y,z)** to computational plane **(** ζ, η, ξ **)** are defined by the following relations :-

$\xi = \xi$ (x,y,z) **…(11-A)**

$\zeta = \zeta$ **(x,y,z)** **…(11-B)**

$\eta = \eta$ **(x,y,z)** **…(11-C)**

The details of transformation is very long and complex, for more details, it is recommended to see **Hoffmann (1989)** and the results are given by:

$$J = \frac{1}{x_\xi\left[y_\eta z_\zeta - z_\eta y_\zeta\right] - x_\eta\left[y_\xi z_\zeta - z_\xi y_\zeta\right] + x_\zeta\left[y_\xi z_\eta - z_\xi y_\eta\right]} \quad \text{…(12)}$$

where J is the jacobian of transformation, and it is defined as the ratio of the volumes in the physical space to that of the computational space. Also the metrics of transformation are given (in 3-D domain) as follows:-

$$\begin{aligned} \xi_x &= J\left[y_\eta z_\zeta - y_\zeta z_\eta\right] & \eta_x &= -J\left[y_\xi z_\zeta - y_\zeta z_\xi\right] \\ \xi_y &= -J\left[x_\eta z_\zeta - x_\zeta z_\eta\right] & \eta_y &= J\left[x_\xi z_\zeta - x_\zeta z_\xi\right] \\ \xi_z &= J\left[x_\eta y_\zeta - x_\zeta y_\eta\right] & \eta_z &= -J\left[x_\xi y_\zeta - x_\zeta y_\xi\right] \end{aligned} \quad \text{…(13-A)}$$

and

$$\begin{aligned} \zeta_x &= J\left[y_\xi z_\eta - y_\eta z_\xi\right] \\ \zeta_y &= -J\left[x_\xi z_\eta - x_\eta z_\xi\right] \\ \zeta_z &= -J\left[x_\xi y_\eta - x_\eta y_\xi\right] \end{aligned} \quad \text{…(13-B)}$$

the physical meaning of the metrics is that, it represents the ratio of arc length in the computational space to that of the physical space. The terms x_ζ , x_η , y_ζ …. are computed numerically using forward approximation, as an example :-

$$y_\eta = \frac{\partial y}{\partial \eta} = \frac{-3y_{i,j,k} + 4y_{i,j+1,k} - y_{i,j+2,k}}{2\Delta\eta} \quad \text{…(14)}$$

6.Numerical Scheme: **E**xplicit time-dependent solution of the three-dimensional Euler equations has been performed using MacCormack's predictor-corrector finite difference technique, which is second-order accurate in both space and time. This method is very effective finite difference technique for viscous and inviscid supersonic flow, specially for unsteady flow shock capturing. By using this technique a computer code is constructed to predict the shock wave which consists from the following steps:

1. a three-dimensional domain is chosen over a arc circular bump, which consists from (**im=21, jm=16** and **km=21**), where:-

im = maximum number of grids in x-direction.
jm = maximum number of grids in y-direction.
km = maximum number of grids in z-direction.

2. a grid generation is performed in (**x-y-z)** direction and the Jacobian and different metrics are calculated.
3. a flow conditions such as **(u,v,w,M,T, e,** ρ and **P)** are computed at the surface **(k=1)** and then they are computed in the domain except at the surface where (I=1 to I=im, j=1 to j=jm, k=2 to k=km).
4. a time step calculation is performed, the time step employed in this work is designed so that it is not exceed the maximum step size permitted by stability. In this study the inviscid **CFL** conditions **AL-Dulaimy (2002)** is used which is given by the following relation: -

$$\Delta t)_{CFL} \le \left[\frac{|u|}{\Delta x} + \frac{|\upsilon|}{\Delta y} + \frac{|w|}{\Delta z} + a * \left[\frac{1}{(\Delta x)^2} + \frac{1}{(\Delta y)^2} + \frac{1}{(\Delta z)^2}\right]^{\frac{1}{2}}\right]^{-1} \quad \text{…(15)}$$

5. a changing of primitive variables to fluxes is occurred which causes to compute the values of flux vectors for all grid points at time step **(n).**
6. a forward predictor version of MacCormack's which is given by **Hoffmann (1989):-**

$$\overline{Q}_{i,j,k}^{n+1} = \overline{Q}_{i,j,k}^{n} - \frac{\Delta t}{\Delta \xi}\left[\overline{E}_{i+1,j,k}^{n+1} - \overline{E}_{i,j,k}^{n+1}\right] - \frac{\Delta t}{\Delta \eta}\left[\overline{F}_{i,j+1,k}^{n+1} - \overline{F}_{i,j,k}^{n+1}\right] - \frac{\Delta t}{\Delta \zeta}\left[G_{i,j,k+1}^{n+1} - G_{i,j,k}^{n+1}\right] \quad \text{…(16)}$$

is used inside the domain where (I=2 to im-1, j=2 to jm-1, k=2 to km-1) where :-

n is the time level **(t)** and **n+1** is the time level **(t+dt).**

7. In order to make our numerical scheme accurate and stable, since we deal with high velocities (high Reynolds number) the following expression for explicit artificial dissipation is added to the predictor step, where $SQ_{i,j,k}^{n+1}$ is a fourth-order artificial viscosity term, defined by **Anderson (1995):-**

$$SQ_{i,j,k}^{n+1} = C_\xi \frac{\left|P_{i-1,j,k}^{n} - 2P_{i,j,k}^{n} + P_{i-1,j,k}^{n}\right|}{P_{i-1,j,k}^{n} + 2P_{i,j,k}^{n} + P_{i-1,j,k}^{n}} * \left[Q_1^{-})_{i-1,j,k}^{n} - 2Q_1^{-})_{i,j,k}^{n} + Q_1^{-})_{i+1,j,k}^{n}\right] +$$

$$C_\eta \frac{\left|P_{i,j-1,k}^{n} - 2P_{i,j,k}^{n} + P_{i,j+1,k}^{n}\right|}{P_{i,j-1,k}^{n} + 2P_{i,j,k}^{n} + P_{i,j+1,k}^{n}} * \left[Q_1^{-})_{i,j-1,k}^{n} - 2Q_1^{-})_{i,j,k}^{n} + Q_1^{-})_{i,j+1,k}^{n}\right] \quad \text{…(17)}$$

$$+ C_\zeta \frac{\left|P_{i,j,k-1}^{n} - 2P_{i,j,k}^{n} + P_{i,j,k+1}^{n}\right|}{P_{i,j,k-1}^{n} + 2P_{i,j,k}^{n} + P_{i,j,k+1}^{n}} * \left[Q_1^{-})_{i,j,k-1}^{n} - 2Q_1^{-})_{i,j,k}^{n} + Q_1^{-})_{i,j,k+1}^{n}\right]$$

The main advantage of artificial dissipation is to provide some mathematical dissipation analogous to the real viscous effects inside the shock wave.

8. A decoding is occurred which is used to produce our parameters from fluxes, also at this step, the contravarient velocity components are computed as :-

$$\mathrm{U} = \xi_x u + \xi_y \upsilon + \xi_z \omega$$

$$\mathrm{V} = \eta_x u + \eta_y \upsilon + \eta_z w \quad \text{…(18)}$$

$$\mathrm{W} = \zeta_x u + \zeta_y \upsilon + \zeta_z w$$

are computed .The contravarient velocity components **U,V** and **W** represent velocity components which are perpendicular to planes of constant ξ , η and ζ

9. A corrector step is computed, where the value of fluxes **(E ,F,G)** are computed at each grid in the intermediate level **(n+1)** depending on the values of primitive variables from previous step, so the computations occurs inside the domain [i=1 to i=im, j=1 to j=jm and k=1 to k=km].
10. a backward corrector version of MacCormack's method which is given by **Fox (1993)** is then applied :-

$$Q_{i,j,k}^{n+1} = (1/2) * \left\{ Q_{i,j,k}^{n} + \overline{Q}_{i,j,k}^{n+1} - \frac{\Delta t}{\Delta \xi}\left[\overline{E}_{i,j,k}^{n+1} - \overline{E}_{i,j-1,k}^{n+1}\right] - \frac{\Delta t}{\Delta \eta}\left[\overline{F}_{i,j,k}^{n+1} - \overline{F}_{i,j-1,k}^{n+1}\right] - \frac{\Delta t}{\Delta \zeta}\left[G_{i,j,k}^{n+1} - G_{i,j-1,k}^{n+1}\right] \right\} \text{…(19)}$$

which is used inside the domain (i=2 to im-1, j=2 to jm-1, k=2 to km-1)and, also a fourth-order artificial viscosity term **Anderson (1995)** at corrector step is added to **Eq.(19)**. This expression is given by:

$$SQ^{n+1})_{i,j,k} = C_\xi \frac{\left|P_{i+1,j,k}^{n+1} - 2P_{i,j,k}^{n+1} + P_{i-1,j,k}^{n+1}\right|}{\left[P_{i+1,j,k}^{n+1} - 2P_{i,j,k}^{n+1} + P_{i-1,j,k}^{n+1}\right]} * \left[\overline{Q}_1)_{i-1,j,k}^{n+1} - 2\overline{Q}_1)_{i,j,k}^{n+1} + \overline{Q}_1)_{i+1,j,k}^{n+1}\right] +$$

$$C_\eta \frac{\left|P_{i,j+1,k}^{n+1} - 2P_{i,j,k}^{n+1} + P_{i,j-1,k}^{n+1}\right|}{\left[P_{i,j+1,k}^{n+1} - 2P_{i,j,k}^{n+1} + P_{i,j-1,k}^{n+1}\right]} * \left[\overline{Q}_1)_{i,j-1,k}^{n+1} - 2\overline{Q}_1)_{i,j,k}^{n+1} + \overline{Q}_1)_{i,j+1,k}^{n+1}\right] \quad \text{…(20)}$$

$$+ C_\zeta \frac{\left|P_{i,j,k+1}^{n+1} - 2P_{i,j,k}^{n+1} + P_{i,j,k-1}^{n+1}\right|}{\left[P_{i,j,k+1}^{n+1} - 2P_{i,j,k}^{n+1} + P_{i,j,k-1}^{n+1}\right]} * \left[\overline{Q}_1)_{i,j,k-1}^{n+1} - 2\overline{Q}_1)_{i,j,k}^{n+1} + \overline{Q}_1)_{i,j,k+1}^{n+1}\right]$$

11. after a corrector step is completed, a decoding step began where our parameters such as (**u,v,w,P,T,e** and **M**) are computed.
12. our parameters are computed under different boundary conditions which can be explained as follows:-

a. up-stream boundary condition(i=1, j=1 to jm, k=1 to km) and at the edge of the body (k=1,i=1, j=1 to jm).

b. solid boundary condition (k=1,i=2 to im ,j=1 to jm)

c. down stream boundary condition (i=im, j=2 to jm-1 and k=2 to km-1).

d. upper plane of symmetry(j=jm, i=2 to im and k=2 to km).

e. plane of symmetry (j =jm, i=2 to im, k=2 to km).

f. far-field boundary condition (k=km, i=1 to im, j=1 to jm).

13.Examining solution convergence, knowing that the last flow field variable to be convergence is the density, therefore, the following convergence criterion was applied at every point in the flow field from one time step to the next **Wylie (1966) :**

$$\text{error} = \frac{\rho_{\text{old}} - \rho_{new}}{\rho_{old}} \leq 1*10^{-8} \qquad \textbf{...(21)}$$

7. RESULTS AND DISCUSSION

Figure (1) shows a mesh generation over a three-dimensional arc circular bump in a moderate supersonic compressible external inviscid flow. The mesh points are produced by using an algebraic grid_generation with (**21** x **16** x **21**) grid points . The explicit technique has required about **(4000)** time steps to achieve the converged solution (steady state solution).In the present work, the artificial viscosity is taken as (**0.5**),as shown in the figure.

Figure (2) shows a Mach number contours for 3D arc circular bump for free stream Mach number **= 1.97**. The shock wave can be noticed clearly. From this figure, the flow pattern near the leading edge of arc circular bump, where the incoming supersonic flow undergoing a sudden change in flow direction resulting a continuous compression wave. The angle of the shock wave depends on arc circular bump shape and free stream Mach number. The shock wave is observed to be detached from circular bump angle and flow behind the shock near the trailing edge of arc circular bump area becomes subsonic. Also, its very important to refer that the clustering process is very necessary near the leading edge of arc circular bump in order to capture all the expected shock waves. This prediction gives a good agreement with the experimental results dealing with the same problem as indicated in **Marsden (2004)**.It is very useful to note that the predicted shock wave by the numerical solution of the current work decelerate the flow speed from supersonic speed up stream of the shock wave to subsonic flow down stream of the shock wave.

Figure (3) shows a temperature contours for supersonic arc circular bump for free stream Mach number =**1.97**.This figure indicates that the temperature distribution occurs at the region between the arc circular bump surface and the shock wave. Also, the temperature increases at the leading edge of arc circular bump due to shock wave strength and is decreased gradually toward its free stream value. The higher temperature can be noticed at the edge of three-dimensional arc circular bump, due to shock wave effect.

Figure (4) shows a pressure contours over a three-dimensional arc circular bump for free stream Mach number =**1.97.** From this figure, the pressure values increases a head of shock wave and then decreased toward its free stream value away from the shock wave. This is agree with **Sorensen (2002)** and **Dietz (2004)** also, the pressure values is increased dramatically near the leading edge of arc circular bump due to shock wave effects.

Figure (5) shows a density contours over a three-dimensional arc circular bump for free stream Mach number =**1.97**. From this figure, the density values increases due to increase of the pressure and this is due to increase in shock wave strength.

Figure (6) shows the internal energy contours over a three-dimensional arc circular bump for free stream Mach number =**1.97**. This figure shows clearly the shock wave prediction and again the internal energy values increases due to shock wave effect. This behavior can be explained as follows:- Since the shock wave decelerate the flow from supersonic speed ahead of the shock wave to subsonic speed down stream of the shock wave. This is certainly causes a reduction in kinetic energy, due to direct proportionality between the flow speed and the kinetic energy and as a result causes an increase in internal energy.

Figures (7) and **(8)** explain the wall pressure profile along an arc circular bump and the historical convergence of numerical simulation of the same problem. The latter figure explains the intermediate solutions of time-dependent schemes. The time level **(n=1)** is the specified initial condition and the figure refers, that at iteration equals **(4000)** the steady state solution is reached. Obviously, this figure just explains a means of reaching to the steady state solution. However, if correct (from physical point of view) and accurate initial data is provided, the solution at various time levels will represent the time dependent solution and it is usually referred to as the **time-accurate solution.**

8. CONCLUSIONS

The following conclusions can be drawn from the results of the present work :-

1. a solution of Euler equation for three-dimensional arc circular bump converges at a range of (**4000**) iteration. The range of iteration is related to the procedure of **grid** producing.
2. for capturing the flow field parameters ; a more mesh points are required near the surface of the arc circular bump.
3. geometry and arc circular bump curvatures have an important effect on the flow field pattern; where in the supersonic flow the change in flow direction due to geometry induced a type of drag. This is called wave drag.
4. since the mesh generation has been separated from explicit solver any mesh type can be used. The stability of the solution depends on the number of grid points and **CFL** condition.
5. the rise in the value of temperature at the **stagnation point** is due to flow nature change from supersonic a head of the shock wave to subsonic down stream of the shock wave. This change will reduce the kinetic

energy and at the same time, this reduction gives an increase in internal energy and as a result increase the temperature.

6. the time-marching solution which is used to deal with a three-dimensional arc circular bump, which can be extended to deal with an axis-symmetry body such as aircraft.
7. from the results obtained, the hydrodynamic properties such as pressure, temperature and density are increased due to shock wave effect
8. the software developed explains, that the convergence depends on the optimum values of the grid points, artificial viscosity and **CFL.**
9. **clustering process** is very necessary at the leading edge of the three-dimensional arc circular bump in order to capture the expected shock wave.

REFERENCES

AL-Dulaimy, F.M., "Numerical Prediction of Supersonic Inviscid and Viscous Flow over Arbitrary Configurations", Ph.D. thesis, University of Technology, Baghdad , 2002.

Hosseini, R. ,Rahimian ,M. and Mirzaei ,M.," Performance of High-Accuracy Schemes in Inviscid Fluxes Calculation " ,Unpublished paper, By **e-mail** from : **hoseinis @ me.ut.ac.ir**.

Hoffmann,A.K.,"Computational Fluid Dynamics for Enginering ", University of Texsas, 1989.

Fox, M. "Supersonic Aerodynamic Characteristic of an Advanced **F-16** Derivative Aircraft Configuration ", NASA Technical Paper 93-3355 , 1993, pp:: 1-22.

Anderson , J.D. ," Computational Fluid Dynamics **,** The Basic with Applications ",McGraw-Hill Book Company , U.S.A., 1995.

Wylie,C.R.," Advanced Engineering Mathematics",International Student Edition , MacGraw -Hill Book Company,U.S.A.,1966.

Marsden,O.,Bogey,C.and Bailly ,C., " Higher-Order Curvilinear Simulations of Flows around Non-Cartesian Bodies", AIAA paper 2004-2813,2004,pp:: 1-15.

Sorensen , N. , " 3D Background Aerodynamics Using CFD ", Riso National Laboratory Publications,Roskilde , Denmark ,2002**,** pp:: 1-18.

Dietz ,W. , Wang ,L., Wenren ,Y., Caradonna , F. and Steinhoff , J. ,"The Development of a CFD-Based Model of Dynamic Stall ",American Helicopter Society , 60 th Annual Forum , Baltimore , U.S.A. , 2004, pp:: 1-17.

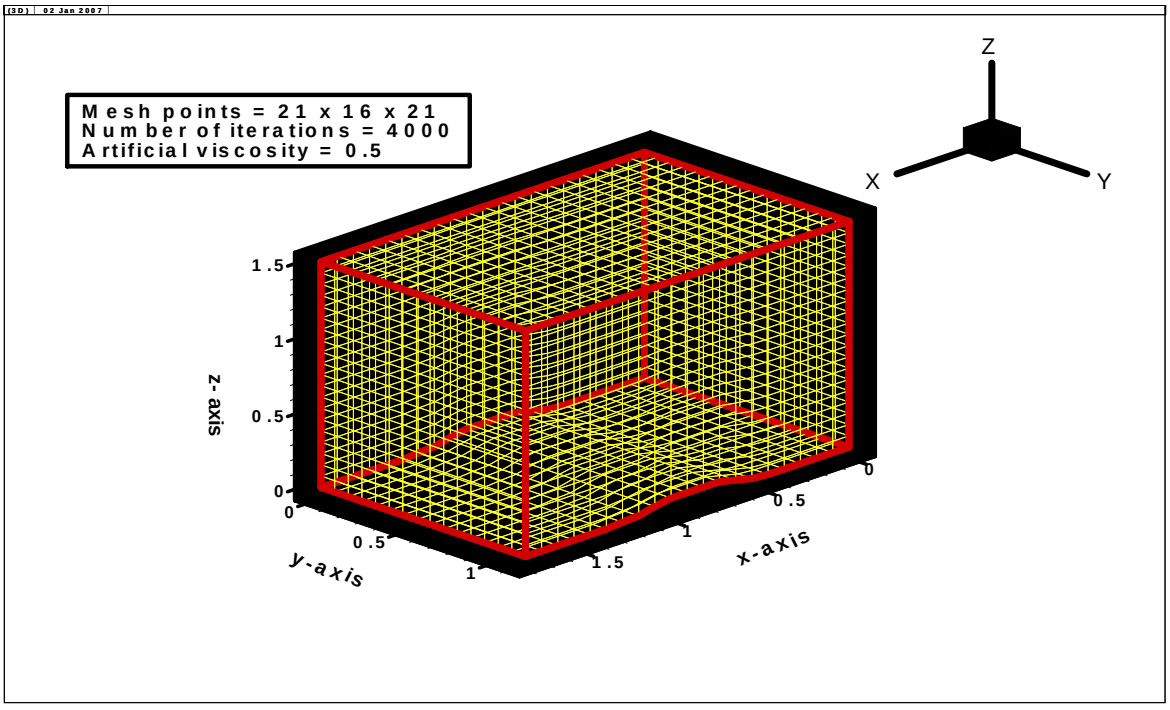

Fig.(1) Algebraic grid generation over a three -dimensional arc circular bump with mesh points (21 x 16 x 21).

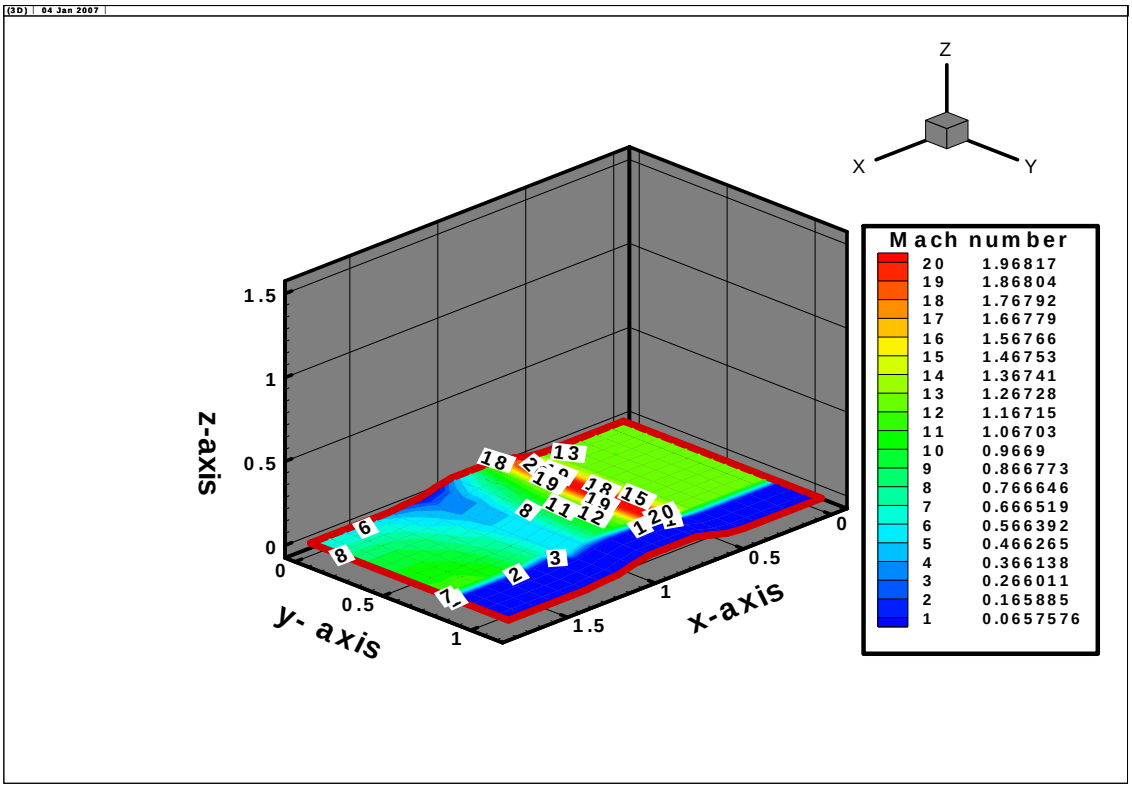

Fig.(2) Mach number contours over a three-dimensional arc circular bump at free stream Mach number = 1.97.

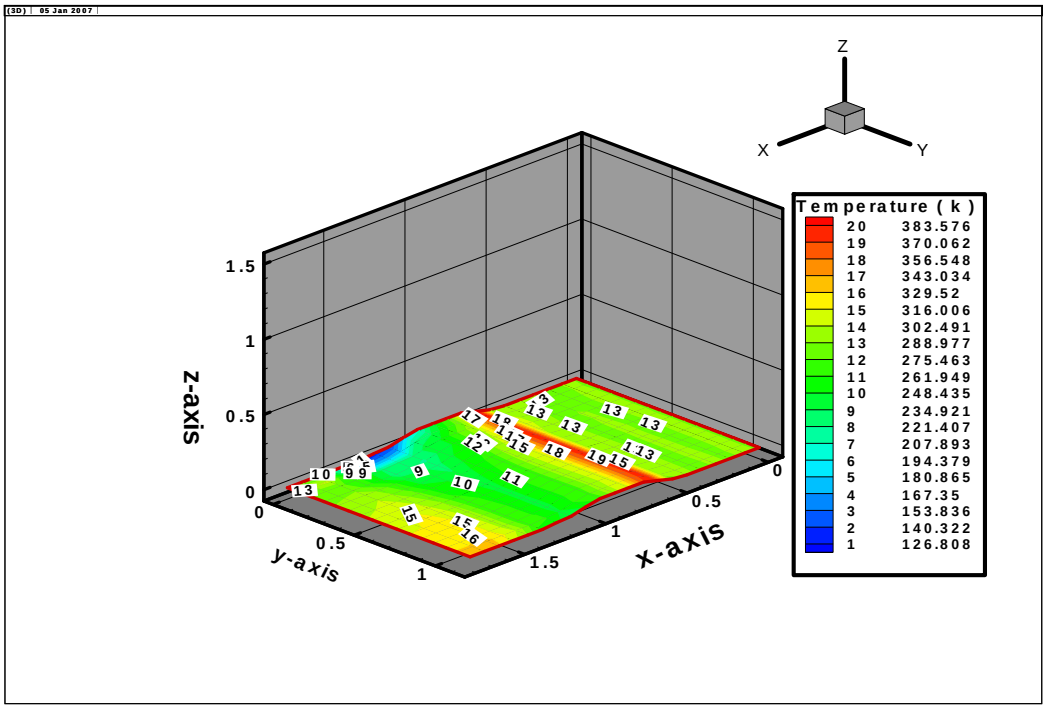

Fig.(3) Temperature contours over a three -dimensional arc circular bump for free stream Mach number = 1.97.

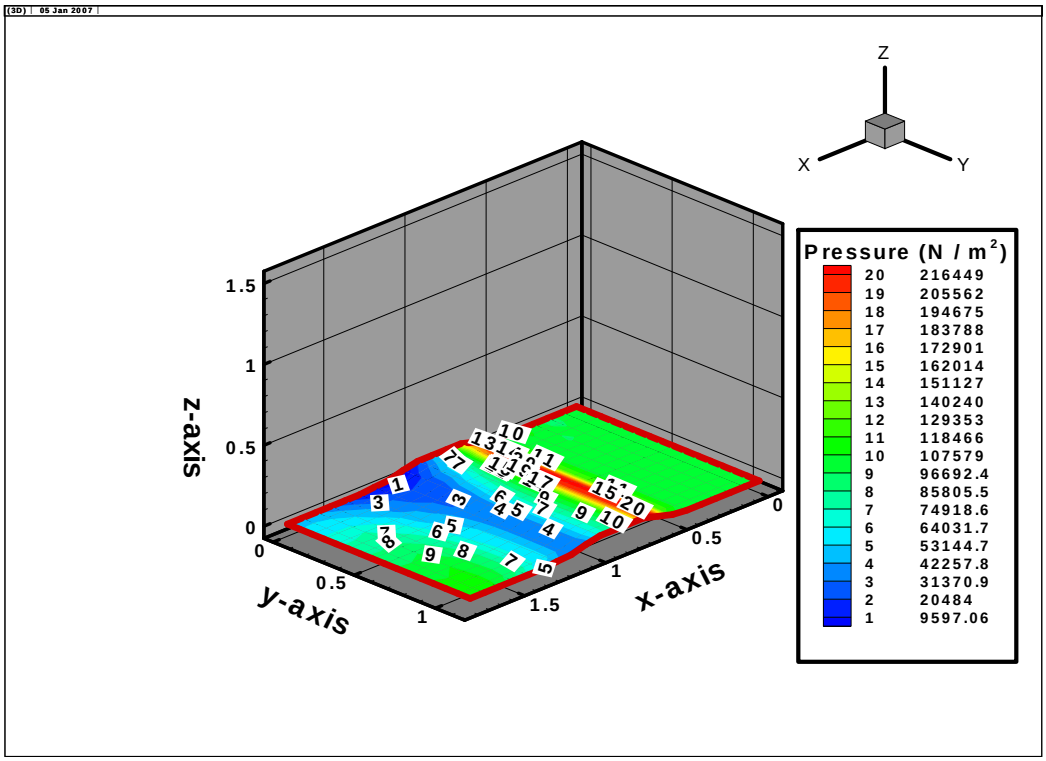

Fig.(4) Pressure contours over a three -dimensional arc circular bump for free stream Mach number = 1.97.

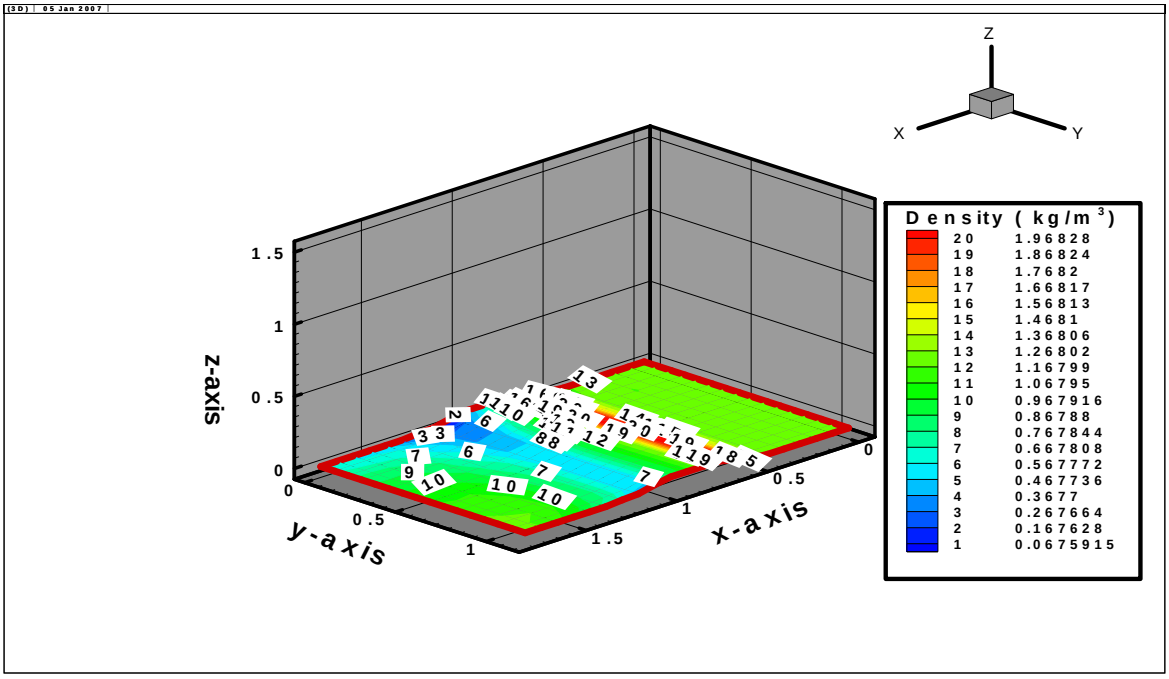

Fig.(5) Density contours over a three- dimensional arc circular bump for free stream Mach number = 1.97.

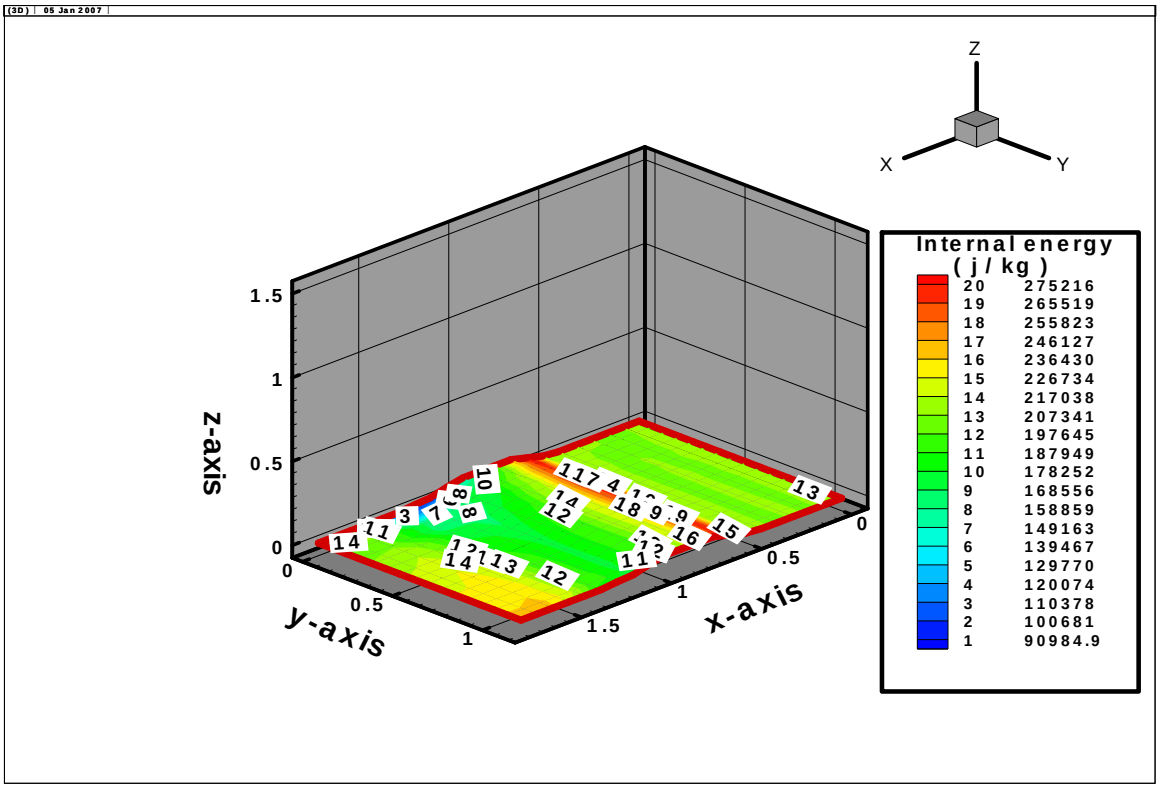

Fig.(6) Internal energy contours over a three dimensional arc circular bump for free stream Mach number = 1.97.

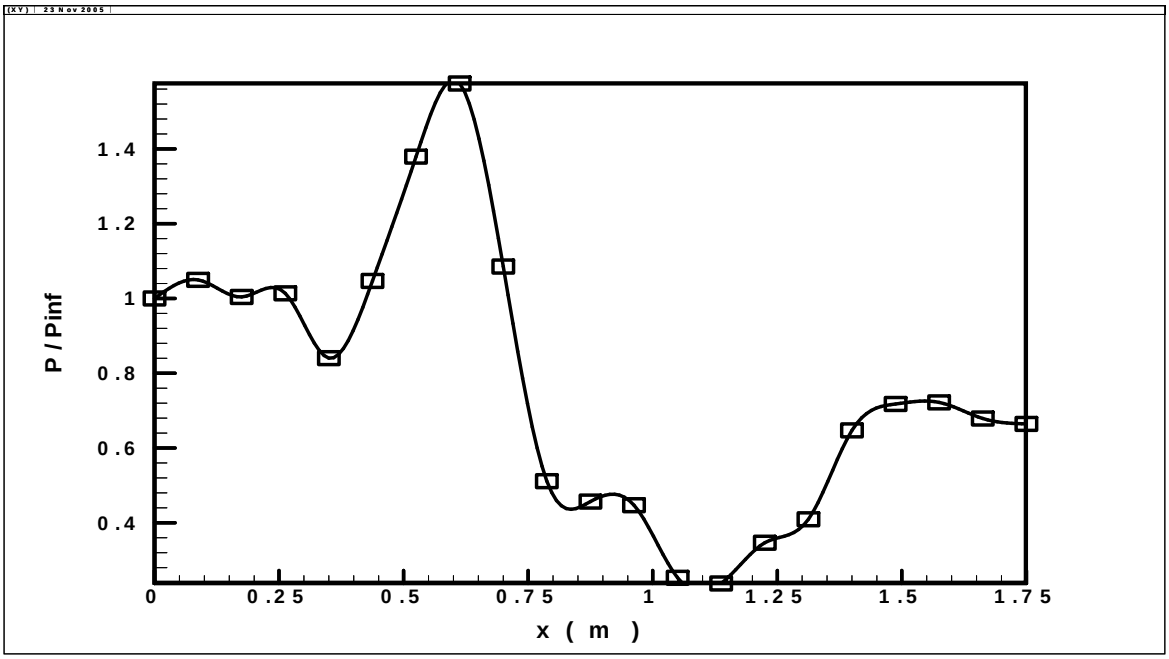

Fig.(7) Wall pressure ratio profile along a three-dimensional arc circular bump for free stream Mach number = 1.97.

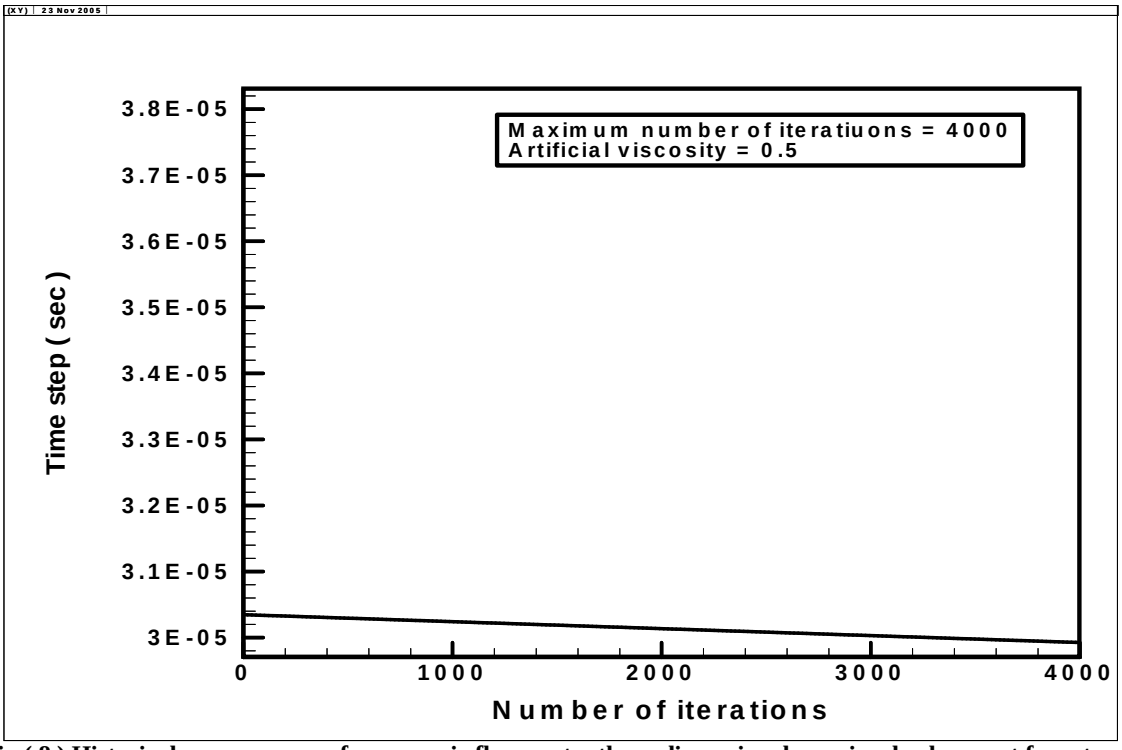

Fig.(8) Historical convergence of supersonic flow past a three-dimensional arc circular bump at free stream Mach number = 1.97.

2. List of Symbols:

Symbol	Description	Dimension
a	Speed of sound.	m/s
CFL	Courant Fridrich Lewys stability condition.	
C_{ξ}, C_{ζ}, C_{η}	Artificial viscosity coefficients in ξ, ζ and η directions respectively.	
e	Specific internal energy per unit mass.	J/kg
E_t	Total energy per unit volume.	J/m^3
E,F,G	Column vector in Cartesian coordinates.	
$\overline{E}, \overline{F}, \overline{G}$	Column vector in body fitted coordinates.	
L	Length of the arc circular bump.	m
J	Jacobian of coordinates transformation.	
M_{∞}	Free stream Mach number.	
P_{∞}	Free stream pressure.	N/m^2
Q	Flux vector.	
$\overline{Q}$	Vector of conserved variable in body fitted coordinates.	
Re	Reynold's number.	
R	Universal gas constant.	J/ kg. K
SQ_1	Artificial viscosity term.	
T_{∞}	Free stream temperature.	K
t	Time.	sec
u	Velocity component in x-direction.	m/s
U	Contravariant velocity component in ξ -direction	m/s
v	Velocity component in y-direction.	m/s
V	Contravariant velocity component in η -direction	m/s
w	Velocity component in z-direction	m/s
W	Contravariant velocity component in ζ -direction	m/s
x , y, z	Cartesian coordinates.	m

Greek Symbols

γ	Ratio of specific heats.	
Δt	Time step.	sec
ρ	Density.	Kg/m^3
α	Angle of attack.	Deg.
δ	Boundary layer thickness.	m
$\Delta x, \Delta y, \Delta z$	Spatial steps in physical domain.	
$\Delta\zeta, \Delta\eta, \Delta\xi$	Spatial steps in computational domain.	
ζ, η, ξ	Computational coordinates.	

Subscript

i, j ,k Node symbols indicates position in x ,y and z directions.

∞ Conditions at free stream.

o Stagnation (total) conditions.

Superscript:

n Time level t .

n+1 Time level $(t + \Delta t)$.